[논문] 수소에너지
J. of the Korean Hydrogen Energy Society
Vol. 10. No. 4(1999)

A Study on the Electrode Characteristics of Hypo-Stoichiometric Zr-based Hydrogen Storage Alloys

Sang-Min Lee, Seoung-Hoe Kim, and Jai-Young Lee

Department of Materials Science and Engineering,
Korea Advanced Institute of Science and Technology,
373-1 Kusong-Dong, Yusong-Gu, Taejon, South Korea

ABSTRACT

The hydrogen storage performance and electrochemical properties of $Zr_{1-x}Ti_x(Mn_{0.2}V_{0.2}Ni_{0.6})_{1.8}$ (X=0.0, 0.2, 0.4, 0.6) alloys are investigated. The relationship between discharge performance and alloy characteristics such as P-C-T characteristics and crystallographic parameters is also discussed. All of these alloys are found to have mainly a C14-type Laves phase structure by X-ray diffraction analysis. As the mole fraction of Ti in the alloy increases, the reversible hydrogen storage capacity decreases while the equilibrium hydrogen pressure of alloy increases. Furthermore, the discharge capacity shows a maxima behavior and the rate-capability is increased, but the cycling durability is rapidly degraded with increasing Ti content in the alloy. In order to analyze the above phenomena, the phase distribution, surface composition, and dissolution amount of alloy constituting elements are examined by S.E.M., A.E.S. and I.C.P. respectively. The decrease of secondary phase amount with increasing Ti content in the alloy explains that the micro-galvanic corrosion by multiphase formation is little related with the degradation of the alloys. The analysis of surface composition shows that the rapid degradation of Ti-substituted Zr base alloy electrode is due to the growth of oxygen

penetration layer. After comparing the radii of atoms and ions in the electrolyte, it is clear that the electrode surface becomes more porous, and that is the source of growth of oxygen penetration layer while accelerating the dissolution of alloy constituting elements with increasing Ti content. Consequently, the rapid degradation (fast growth of the oxygen-penetrated layer) with increasing Ti substitution in Zr-based alloy is ascribed to the formation of porous surface oxide through which the oxygen atom and hydroxyl ion with relatively large radius can easily transport into the electrode surface.

Introduction

Nickel-metal hydride (Ni-MH) batteries using hydrogen storage alloys as the negative electrode have been developed and commercialized to meet strong market demand for a power source with high energy density, high rate capability, long cycle life, and better environmental compatibility. A number of metals, alloys, and intermetallic compounds capable of forming hydrides have been studied extensively as a potential electrode, among which the rare earth metal-based and Ti or Zr-based alloys are considered to be most promising.1,2 However, rare earth metal and Ti-based alloys are limited in developing high-capacity and high-performance Ni/MH batteries, because these alloys have a small discharge capacity and a poor cycle life, respectively. 3,4 The Zr-based Laves phase hydrogen-storage alloys have become known as new, promising negative electrode materials for Ni-MH batteries to replace rare-earth alloys because of much higher discharge capacity.5 Investigation of the performance of Laves phase hydrogen-storage alloys as negative electrodes has been actively pursued ; for example, the discharge capacity has been optimized by substituting various metals as partial constituents and by deviating the composition ratio from stoichiometry. 6

However, most of them had a low surface reaction kinetics (e.g., rate-capability, activation properties, etc.) compared with the conventional mixed rare-earth metal (Mm)Ni5-based alloys. The surface catalytic activity of the Zr-based alloy has been improved by the chemical modification of surface, such as the F-treatment, ball-milling process, etc.7,8 The surface modification methods have disadvantages of toxic process, shortage of reproducibility making them impossible to apply for commercialization. On the other hand, it has been reported recently that some Ti-substituted Zr-base Laves phase alloys showed remarkably improved kinetic properties compared to Zr-based alloy.9 A mixture of titanium and zirconium oxides should be much less of a barrier to hydrogen penetration compared with a pure zirconium oxide layer. In this work, in order to develop

the hydrogen storage alloy with higher discharge capacity and rate-capability, the hypo-stoichiometric Zr-based Laves phase alloys substituted by Ti are investigated. The changes of thermodynamic/electrochemical properties of the alloy with the variation of Ti mole fraction will be discussed on the basis of phenomenological/electrochemical analyses.

Experimental

The base alloy was prepared in an arc-melting furnace under an argon atmosphere. The purity of the metals was at least 99.5 weight percent (w/o). To assure the homogeneity of the alloy, the alloy ingot was turned over and remelted at least 5 times. The samples were crushed and ground into a powder with a characteristic particle diameter of about 100m for measurement of P-C-Isotherms and a particle diameter less than 45m for electrochemical measurements. For the electrochemical measurement, electrodes were made by mixing the sieved powders with copper powder in a weight ratio of 5:1 and pressing this mixtures at a pressure of 104 N/m2 to porous pellets having a diameter of 10mm. The experimental cell for electrochemical measurements consisted of the working electrode (Metal Hydride electrode), the counter electrode (Pt wire) and a reference electrode (Hg/HgO electrode). The reference electrode was equipped with a Luggin probe to reduce the IR drop in the polarization measurements. The electrolyte was 30wt% KOH solution and its temperature was controlled at 30 ±1℃, The alloy electrode was galvanostatically charged at 100mA/g for 6h, and after resting for 5min it was discharged at 100mA/g until the potential reached -0.75V vs. Hg/HgO. To examine the reason for the change of discharge behavior during cycling, the phase distribution of the alloy was analyzed by scanning electron microscopy (S.E.M.) and its chemical composition was characterized by energy dispersive spectroscopy (E.D.S.) analysis. The electrochemical impedance spectra for cycled electrodes were recorded out under open-circuit conditions using a Solartron SI1255 frequency response analyzer and a EG&G 273A potentiostat. The impedance spectra of the electrodes were recorded in a frequency range from 10KHz to 5mHz and at 5mV of amplitude perturbation for constant depth of discharge (DOD=50%). Furthermore in order to analyze the surface composition of the alloy after electrochemical cycling, Auger electron spectroscopy (A.E.S.) analysis was performed. In A.E.S. analysis, a Perkin-Elmer PHI4300-SAM instrument having a base pressure of 1 x 10-9 torr was used and depth profiling was performed by using Ar^+ ions at 3kV for sputtering. I.C.P.(Inductively Coupled Plasma) analysis was carried out to investigate the dissolved amount of each constituent element in KOH electrolyte during electrochemical cycling.

Results and discussion

Discharge characteristics of $Zr_{1-x}Ti_x(Mn_{0.2}V_{0.2}Ni_{0.6})_{1.8}$ (X=0.0, 0.2, 0.4, 0.6) alloys - Figure 1 shows the discharge curves at 30℃ for $Zr_{1-x}Ti_x(Mn_{0.2}V_{0.2}Ni_{0.6})_{1.8}$ (X=0.0, 0.2, 0.4, 0.6) alloy electrodes with respect to Ti content. It is seen in this figure that the electrochemical discharge capacity passes through a maximum with Ti content in the alloys.

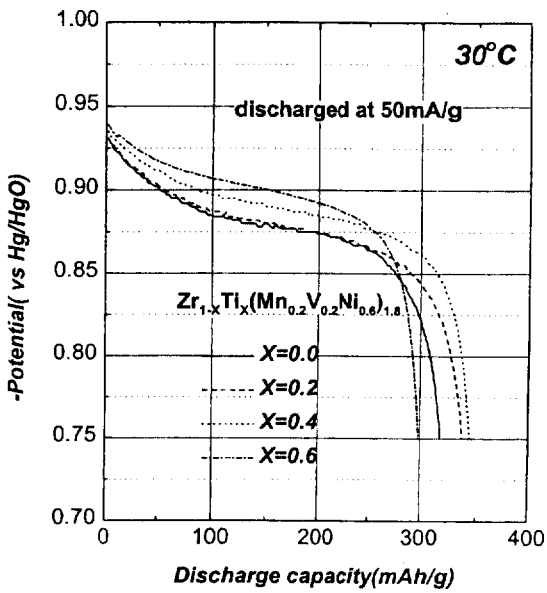

Fig. 1. The discharge curves at 30℃ for $Zr_{1-x}Ti_x(Mn_{0.2}V_{0.2}Ni_{0.6})_{1.8}$ (x=0.0, 0.2, 0.4, 0.6) alloy electrodes with respect to Ti contents.

Measurement of P-C-T(Pressure-Composition) Isotherm curves - To analyze the above phenomena, the PCT curves were measured for the $Zr_{1-x}Ti_x(Mn_{0.2}V_{0.2}Ni_{0.6})_{1.8}$ (X=0.0, 0.2, 0.4, 0.6) alloys. Typical pressure- composition isotherms of the $Zr_{1-x}Ti_x(Mn_{0.2}V_{0.2}Ni_{0.6})_{1.8}$ (X=0.0, 0.2, 0.4, 0.6) alloys are illustrated in Fig. 2. It appears that the equilibrium hydrogen pressure increases, but the reversible hydrogen storage capacity absorbed in 0.01- 1 atm range of equilibrium hydrogen pressure decreases with increasing Ti mole fraction(X).

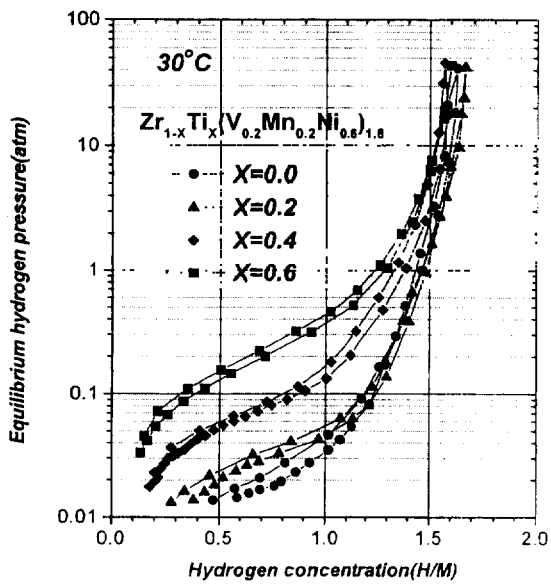

Fig. 2. The Pressure-composition isotherms of $Zr_{1-x}Ti_x(Mn_{0.2}V_{0.2}Ni_{0.6})_{1.8}$ (X=0.0, 0.2, 0.4, 0.6) alloys at 30℃.

Crystallographic structure identified by X-ray Diffraction analysis - In general, the hydrogen storage capacity and the hydrogen equilibrium pressure of alloy are

closely related to the size of hydrogen sites(i.e. tetrahedral interstices) and the change of the chemical affinity of alloy for hydrogen. The crystal structure and the size of hydrogen sites(i.e. tetrahedral interstices)of $Zr_{1-x}Ti_x(Mn_{0.2}V_{0.2}Ni_{0.6})_{1.8}$ (X=0.0, 0.2, 0.4, 0.6) alloys were investigated by XRD analysis. From the XRD results shown in Fig. 3(a), it is found that the alloys have a main hexagonal C14 Laves phase and a very small amount of second phase identified to be Ti-Zr-Ni phase. Considering the change of X.R.D. patterns with increasing Ti mole fraction, it is predicted that the amount of second phase(Ti-Zr-Ni) slightly decreases.

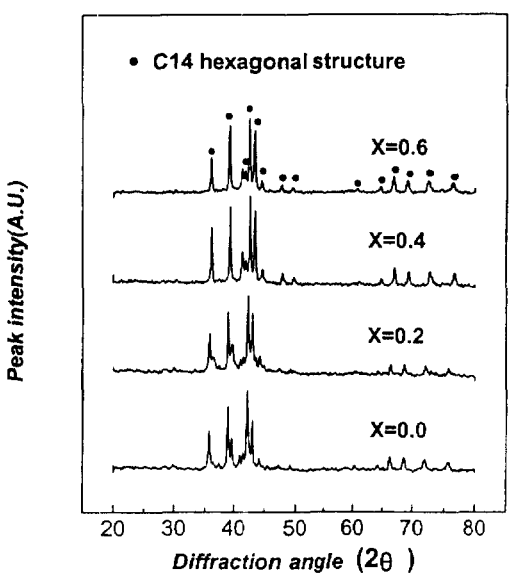

Fig. 3(a). X-ray diffraction patterns of $Zr_{1-x}Ti_x(Mn_{0.2}V_{0.2}Ni_{0.6})_{1.8}$ (X=0.0, 0.2, 0.4, 0.6) alloys.

On the other hand it is also observed in Fig. 3(b) that the lattice parameters decrease with the increasing amount of substituted Ti. This means that both the lattice volume and the size of hydrogen sites(i.e. tetrahedral interstices) decreases. Therefore it seems that the increase of the hydrogen equilibrium pressure and the decrease of the hydrogen storage amount is attributed to the lattice shrinkage and the change in chemical affinity for hydrogen of the metals.

Nevertheless, the hydrogen storage capacity decreases and the electrochemical discharge capacity passes through a maximum with increasing Ti content. Therefore, it is thought that there exists another factor affecting the electrochemical discharge capacity. This factor is supposed to be the discharge kinetics, i.e. the rate-capability.

Measurement of rate-capability for $Zr_{1-x}Ti_x(Mn_{0.2}V_{0.2}Ni_{0.6})_{1.8}$ (X=0.0, 0.1, 0.2, 0.3, 0.4) - Fig. 4 shows the rate-capabilities of for $Zr_{1-x}Ti_x(Mn_{0.2}V_{0.2}Ni_{0.6})_{1.8}$ (X=0.0, 0.1, 0.2, 0.3, 0.4) alloys for various Ti contents at 30℃. As expected, the rate-capability increases as the amount of substituted Ti increases. Therefore the maxima phenomenon of the electrochemical discharge capacity of the alloy is attributed to a competition between decreasing hydrogen storage capacity and increasing of rate-capability with increasing Ti content. On the other hand, the increase of the rate-capability of this alloy system with increasing Ti content may be due to the formation of a

Ti-oxide film on the MH surface, which is believed to be more porous than the Zr-oxide film and to let the hydrogen penetrate easily through its porous surface.

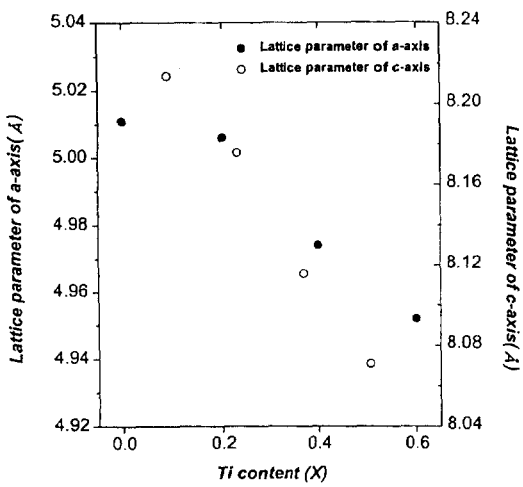

Fig. 3(b). The change of lattice parameter (lattice parameters of A-axis and C-axis in the figure are denoted as closed circle and open circle symbol, respectively)of $Zr_{1-x}Ti_x(Mn_{0.2}V_{0.2}Ni_{0.6})_{1.8}$ (X=0.0, 0.2, 0.4, 0.6) alloys with respect to Ti contents in the alloy.

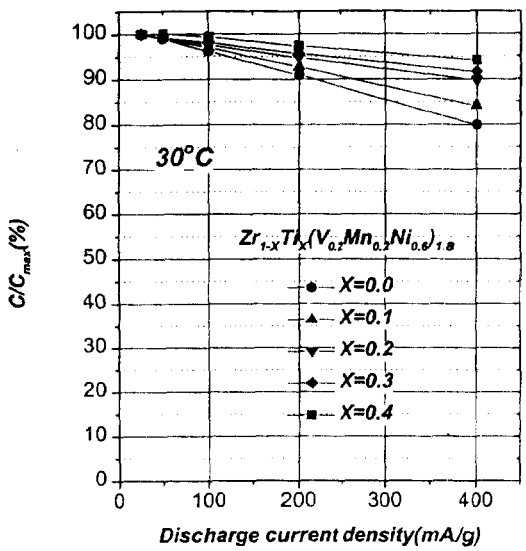

Fig. 4. The change of discharge capacity of $Zr_{1-x}Ti_x(Mn_{0.2}V_{0.2}Ni_{0.6})_{1.8}$ (X=0.0, 0.2, 0.4, 0.6) alloy electrodes with increasing discharge current density.

Measurement of cycle life for $Zr_{1-x}Ti_x(Mn_{0.2}V_{0.2}Ni_{0.6})_{1.8}$ (X=0.0, 0.2, 0.4, 0.6) - The cycle life of $Zr_{1-x}Ti_x(Mn_{0.2}V_{0.2}Ni_{0.6})_{1.8}$ (X=0.0, 0.2, 0.4, 0.6) alloy electrodes is illustrated graphically in Fig. 5 by plotting the ratio of discharge capacity to the maximum discharge capacity, C/Cmax, vs. cycles. Inspection of the individual plots reveals the general behavior. There is an initial steep increase in capacity in the first few cycles; this comprises the activation process which consists of particle size PV reduction and surface reconstruction. After activation, a maximum in electrochemical storage

capacity, Cmax is reached. This is usually followed by essentially linear decrease in capacity as a function of cycles which may be termed capacity decay. As Ti mole fraction increases, the discharge capacity decreases more rapidly with repeated electrochemical cycling. In general, it is reported that the degradation mechanisms of AB2 type Laves phase hydrogen storage alloy electrodes are classified as follows; degradation of surface properties by oxygen penetration10, degradation of bulk properties by micro-galvanic corrosion11. To find out the reason why more rapid degradation occurs with increasing Ti mole fraction in Ti-substituted Zr-base alloy, we intend to examine which acts as a dominant mechanism in the degradation of alloy in view of degradation mechanisms depicted generally.

Phase analysis of $Zr_{1-x}Ti_x(Mn_{0.2}V_{0.2}Ni_{0.6})_{1.8}$ (X=0.0, 0.2, 0.4, 0.6). - First of all, to identify whether the micro-galvanic corrosion by multiphase formation should be a main source for degradation of Ti-substituted Zr-base alloy electrodes with increasing Ti mole fraction, the phase morphologies of alloys was analyzed by S.E.M. The cross-sectional images of the alloys are shown in Fig. 6. The amount of secondary phase is reduced with the content (X) of Ti and disappeared above X=0.4. The secondaryphase is identified as Ti-Zr-Ni phase from E.D.S. analysis. It is noticeable that the amount of secondary phase decreases with the mole fraction of Ti in the alloys increases, which is contrary to the degradation behavior of the alloy electrodes. It implies that the micro-galvanic corrosion by multiphase formation is little related with the degradation of the alloys but some other factors may have influences on the degradation like the change of surface properties on the alloys caused by oxygen diffusion or penetration.

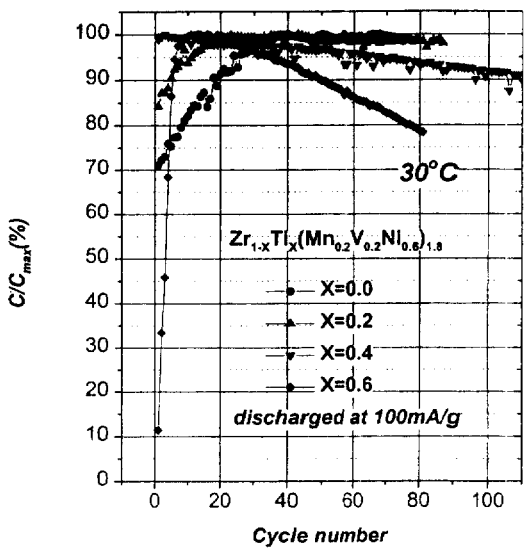

Fig. 5. The cycle life curves of $Zr_{1-x}Ti_x(Mn_{0.2}V_{0.2}Ni_{0.6})_{1.8}$ (X=0.0, 0.2, 0.4, 0.6) alloy electrodes at discharge current density of 100mA/g.

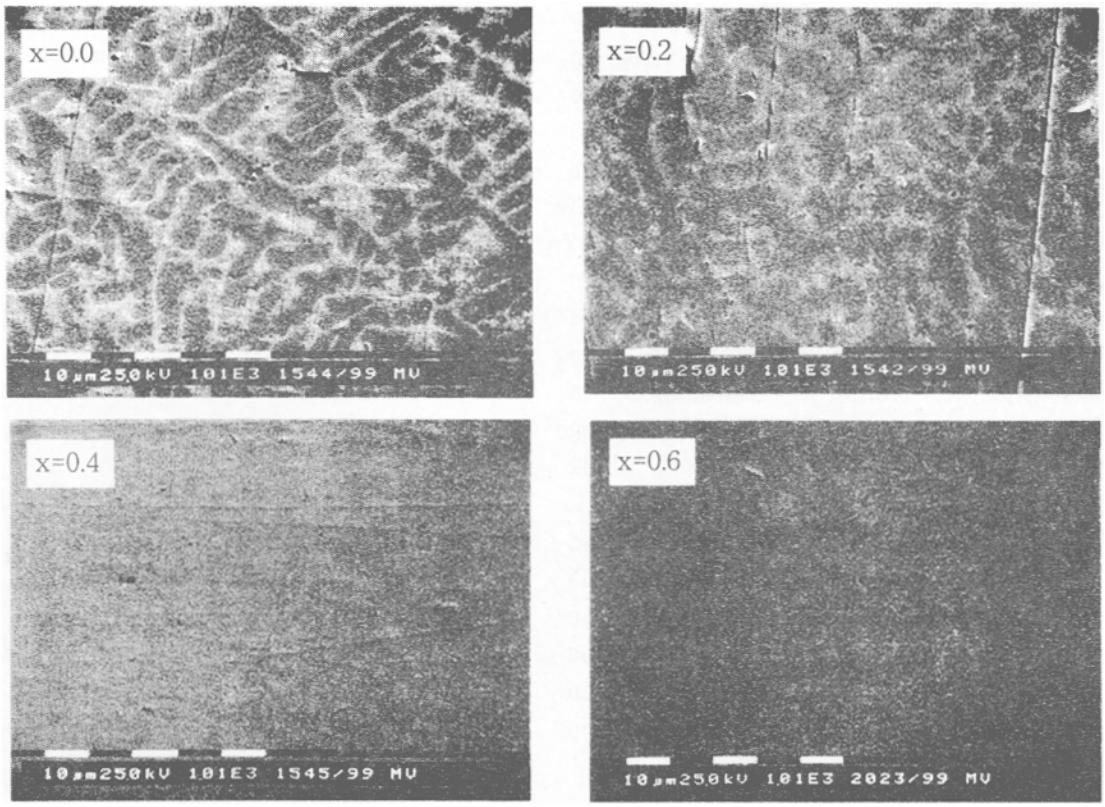

Fig. 6. The cross-sectional view of $Zr_{1-X}Ti_X(Mn_{0.2}V_{0.2}Ni_{0.6})_{1.8}$ (a) X=0.0, (b) X=0.2, (c) X=0.4, (d) X=0.6 alloy imaged by S.E.M.

Electrochemical Impedance Spectroscopy analysis - The changes of impedance spectra of $Zr_{1-X}Ti_X(Mn_{0.2}V_{0.2}Ni_{0.6})_{1.8}$ (X= 0.2, 0.4, 0.6) alloy electrodes from 10KHz to 5mHz at the constant depth of discharge (DOD=50%) during cycling are shown in Fig. 7 (a),(b),(c). The Cole-Cole plots almost consist of two obvious semicircles. In the case of Zr-based alloy electrode substituted with higher Ti content, the smaller semicircle in the high-frequency region(; contact resistance between alloy particles) is hardly changed, but the semicircle in the low-frequency region(; charge transfer resistance for hydrogenation reaction) is changed markedly during cycling12. The phenomena mean that the rapid degradation of Ti-substituted Zr-base alloy electrode is ascribed to the increase of charge transfer resistance during cycling.

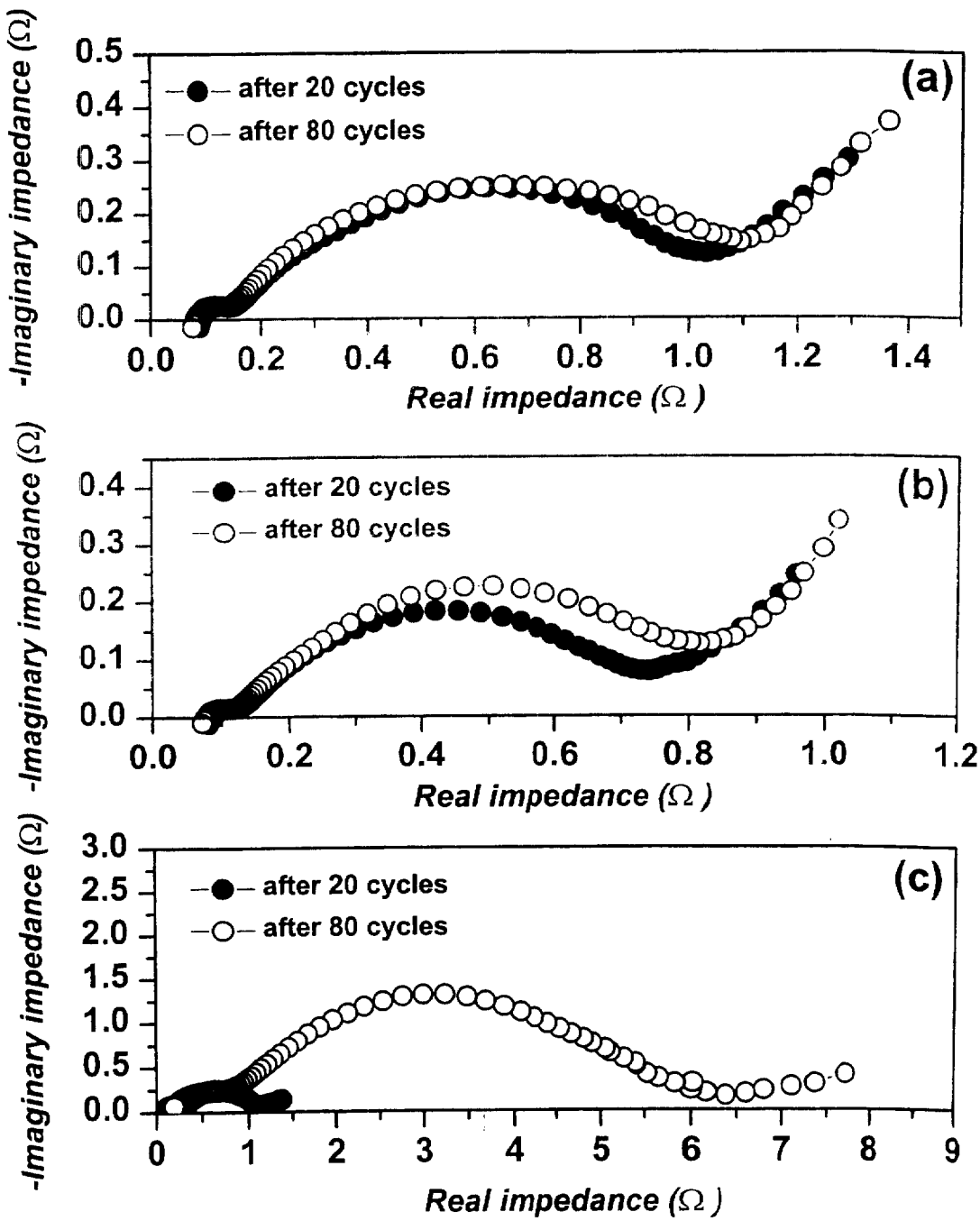

Fig. 7. Cole-Cole plots for $Zr_{1-x}Ti_x(Mn_{0.2}V_{0.2}Ni_{0.6})_{1.8}$ alloy electrodes (a) X=0.2, (b) X=0.4 and (c) X=0.6 at constant applied D.O.D = 50%

Alloy surface composition analysis - In order to identify the variation in the surface properties of the alloys, A.E.S. analyses are performed as shown in Fig. 8. It is observed that the surface composition of alloy electrode with higher Ti mole fraction is characterized by the higher oxygen concentration. It demonstrates that the degradation of Ti-substituted alloy electrode is caused by the penetration of oxygen into the alloy surface during cycling.

Figure 9 (a) shows the Auger spectrum of $Zr_{0.4}Ti_{0.6}(Mn_{0.2}V_{0.2}Ni_{0.6})_{1.8}$ with sputter depth profiling time. Surprisingly, the penetration of potassium (K or K+), which may be originated from KOH electrolyte, is also observed in the surface inner region. On the other hand, if the sputtering yield of each alloy electrode is assumed to be similar when performed by A.E.S., the Auger spectrum of $Zr_{0.8}Ti_{0.2}(Mn_{0.2}V_{0.2}Ni_{0.6})_{1.8}$ with sputter depth profiling time indicates that the K or K+ hardly penetrates into the electrode surface region (Fig. 9 (b).

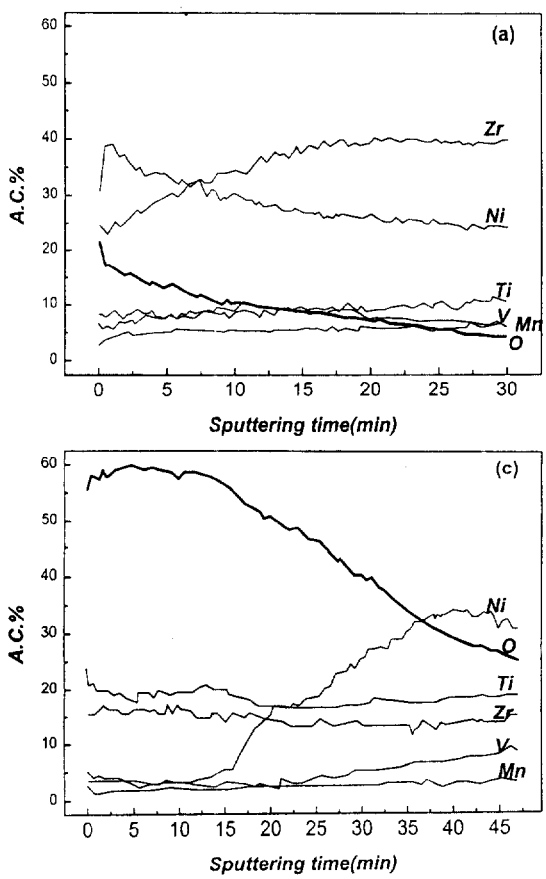

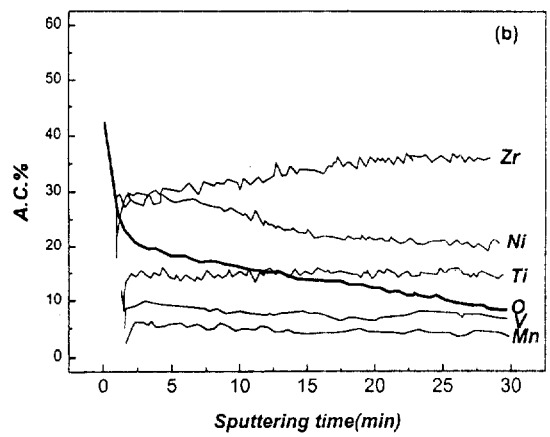

Fig. 8. A.E.S. depth profiles for the constituent elements of (a) X=0.2, (b) X=0.4, (C) X=0.6 in the $Zr_{1-x}Ti_x(Mn_{0.2}V_{0.2}Ni_{0.6})_{1.8}$ alloy electrodes after 80 cycles.

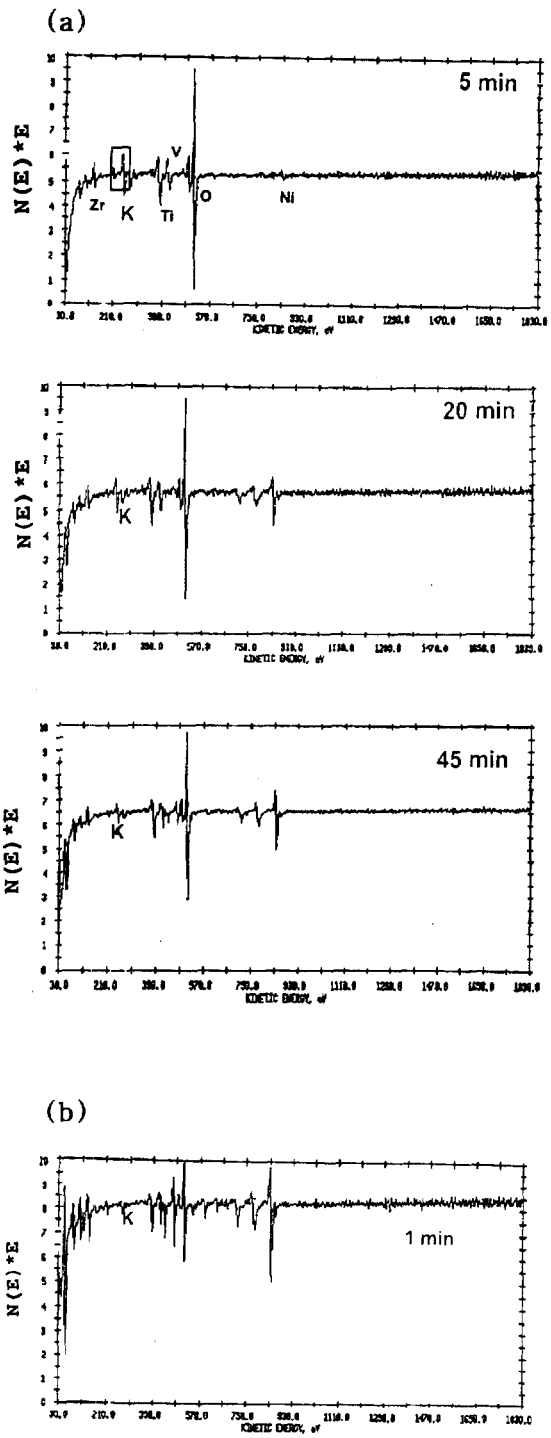

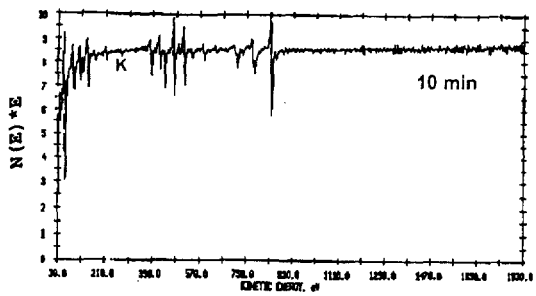

Fig. 9. Auger spectra with sputter depth profiling time of
(a) $Zr_{0.4}Ti_{0.6}(Mn_{0.2}V_{0.2}Ni_{0.6})_{1.8}$
(b)$Zr_{0.8}Ti_{0.2}(Mn_{0.2}V_{0.2}Ni_{0.6})_{1.8}$
alloy electrodes after 80 cycles.

Discussion - Considering the deep penetration of K or K+ into the electrode surface of higher Ti-substituted Zr-base alloy, it is supposed that some other atoms or ions in the electrolyte can be penetrate into the electrode surface. Comparing the radii of various atoms and ions in the electrolyte (Table 1), the radii of hydroxyl ion (OH-) and oxygen atom(O), which are sources of corrosion and oxidation reactions produced during electrochemical cycling, are smaller than that of K or K+ 13. It implies that the hydroxyl ion (OH-) and oxygen atom(O) can penetrate into the electrode surface of Ti-substituted Zr-base alloy. In general, it is well known that the corrosion and oxidation reactions can be the origin of oxygen penetration into the alloy surface in contact with aqueous electrolyte. Lee *et al* reports that the corrosion of Ti based alloy is accompanied by dissolution of alloy constituting elements like V, Mn,

etc. Therefore, to examine the possibility of penetration of OH- causing metal corrosion in the solid/aqueous electrolyte reaction, the dissolved amount of alloy constituting elements is measured by I.C.P. analysis (Fig. 10). The dissolution of the elements, especially Zr, Ti, V, Mn, is observed in the electrolyte after 80cycles. The dissolved amount of Ti, Mn, Zr elements is slightly changed but that of V is strikingly increased with increasing Ti mole fraction in the Zr-based alloy. It indicates that the hydroxyl ion is penetrated into the alloy surface after cycling. Therefore, it can be suggested that the surface oxide region of Ti-substituted Zr-base alloy gets more porous with increasing Ti mole fraction. The porous structure of surface oxide film of Ti-substituted Zr-base alloy may lead to the oxygen penetration and also to dissolution of alloy constituting elements through oxide film. From the above results, it can be summarized as follows ; the rapid degradation (fast growth of the oxygen-penetrated layer) with increasing Ti content in Zr-based alloy is ascribed to the formation of porous surface oxide through which the oxygen atom and hydroxyl ion with relatively large radius can easily transport into the electrode surface.

Table1. The comparison of atomic and ionic radii in the KOH electrolyte13.

	K	K+	OH-	O
Radii of atom and ion ()	2.31	1.33	1.30	0.65 - 0.73

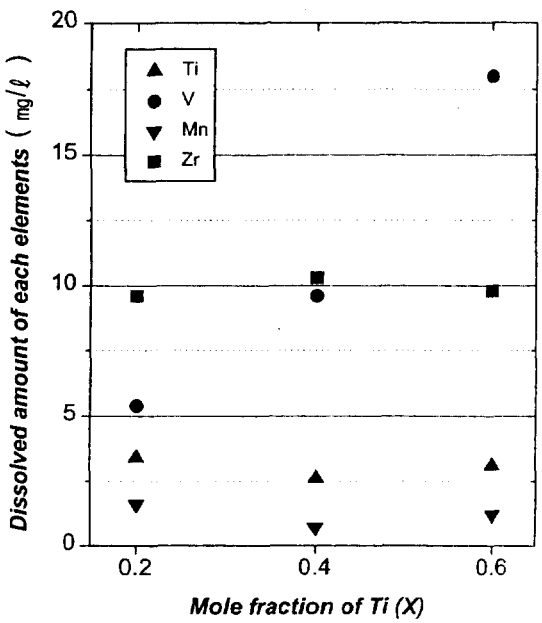

Fig. 10. The dissolved amount of each constituting elements into the electrolyte for $Zr_{1-x}Ti_x(Mn_{0.2}V_{0.2}Ni_{0.6})_{1.8}$ (X=0.2, 0.4, 0.6) alloy electrodes after 80 cycles

Conclusions

The electrode characteristics of hypo-stoichiometric $Zr_{1-x}Ti_x$ $(Mn_{0.2}V_{0.2}Ni_{0.6})_{1.8}$ (X=0.0, 0.2, 0.4, 0.6) alloys have been investigated. As the mole fraction of Ti is increased in the Zr-based alloy, the total hydrogen storage capacity decreases, but the change of reversible hydrogen storage capacity shows maximum behavior. These phenomena can be attributed to the lattice shrinkage and the change of chemical affinity for hydrogen of the metals. In addition, the rate-capability also increases with increasing Ti content in the alloy. Consequently,. the maxima phenomenon of the electrochemical discharge capacity of the alloy is attributed to a competition between decreasing hydrogen storage capacity and increasing of rate-capability with increasing Ti content. However, the discharge capacity gets more rapidly decreased with repeated electrochemical cycling for the higher Ti-substituted Zr-base alloy. It is found that the increase of charge transfer resistance of alloy electrode is more significant during cycling with increasing Ti content as determined by E.I.S. analysis. The surface analysis shows that the rapid degradation of Ti-substituted Zr-base alloy electrode is caused by the penetration of oxygen into the alloy surface during cycling. In other words, the surface oxide region of Ti-substituted Zr-base alloy gets more porous with increasing Ti mole fraction. The porous structure of surface oxide film of Ti-substituted Zr-base alloy may lead to the oxygen penetration and also to dissolution of alloy constituting elements through oxide film. Consequently, the rapid degradation (fast growth of the oxygen-penetrated layer) with increasing Ti substitution in Zr-based alloy is ascribed to the formation of porous surface oxide through which the oxygen atom and hydroxyl ion with relatively large radius can easily transport into the electrode surface.

Acknowledgments

This work was conducted under the Research and Development programs on a development of metal hydride anode for high performance secondary battery in the projects sponsored by the Ministry of Science and Technology (MOST) and Dekeun Industrial Co., Ltd.

REFERENCES

1. J. J. Willems and K. H. J. Buschow, *J. Less-Common Metals*, 129, 13 (1987).
2. M. A. Fetchenko, S. Venkatesan, K. C. Hong, B. Beichman, *Power Sources*, 12, 411 (1989).
3. P. H. L. Notten, and P. Hokkeling, *J. Electrochem. Soc.*, 138, 1877 (1991).
4. H. H. Lee, J. Y. Lee, *J. Alloys and Compounds*, 253, 601 (1997).
5. S. Fujitani, I. Yonezu, T. Saito, N. Furukawa, E. Akiba, H. Hayakawa, and S. Ono, *J. Less-Common Met.*, 172-174, 220 (1991).
6. D. M. Kim, S. W. Jeon, and J. Y. Lee, *J. Alloys and Compounds*, 253, 601 (1997).
7. X. P. Gao, W. Zhang, H. B. Yang, D. Y. Song, Y. S. Zhang, Z. X. Zhou, and P. W. Shen, *J. Alloys and Compounds*, 235, 225 (1996).
8. Dalin Sun, M. Latroche, and A. Percheron-Guegan, *J. Alloys and Compounds*, 257, 302 (1997).
9. A. Zttel, F. Meli, and L. Schlapbach, *J. Alloys and Compounds*, 231, 645 (1995).
10. S. R. Kim, K. Y. Lee, and J. Y. Lee, *J. Alloys and Compounds*, 223, 22 (1995).
11. H. Lee, S. M. Lee, and J. Y. Lee, *J. Electrochem. Soc.*, 146, (10) 3666-3671 (1999)
12. N. Kuriyama, T. Sakai, H. Miyamura, I. Uehara and H. Ishikawa, *J. Alloys and Compounds*, 192, 161 (1993).
13. David R. Lide (Editor-in-Chief) in *CRC Handbook of Chemistry and Physics*, CRC Press, New York 12-14 (1995)